Materials and Methods

Materials and reagent

The fresh buckwheat flour was purchase from Sichuan province of China. Nafion solution, carbon black, polyvinylidene fluoride (PVDF), N-methylpyrrolidone (NMP) were purchased from Sigma-Aldrich. Potassium hydroxide (KOH) and all others reagents were obtained from Adamas-beta®. All chemicals were used without further purification.

Synthesis of honeycomb-like porous carbon foam (HPC)

HPC (Figure S2b-c) was manufactured via a facile one-step pyrolysis of the mixture of buckwheat flour precursor and KOH. Typically, buckwheat flour and KOH were firstly mixed with a mass ratio of 2:1 in 40 mL deionized water, and then dried at 80 ℃ for 12 h. The resulting product was heated in a tubular furnace under argon gas at 700 ℃ for 2 h with a heating rate of 3 ℃ min^{-1}. Then, the product was washed with dilute HCl solution and distilled water, and dried at 80 ℃ for 12 h in a vacuum oven. As a contrast, the different mass ratios of wheat flour and KOH (1:2, 1:1, 2:3) were also investigated under the above-mentioned process. Additionally, buckwheat flour was heated at 700 ℃ for 2 h under the similar condition, and the as-obtained carbon was named as CF (Figure S2a). Then CF and KOH with a mass ratio of (1:2 or 1:1 or 2:1) were thoroughly ground in an agate mortar, heated at 700 ℃ for 2 h according to the analogous procedure, and the as-obtained carbon was denoted as ACF. All carbonized samples were thoroughly washed with dilute HCl and deionization water, and dried at 80 ℃ for 12 h.

Characterizations

The XRD patterns of all samples were recorded using powder X-ray diffraction (Shimadzu XRD-7000). The surface morphology and structure of samples were observed using scanning electron

microscopy (FESEM, JSM-7800F) and transmission electron microscopy (TEM, JEOL 2100). Nitrogen sorption isotherms were obtained using an Autosorb-1 (Quantachrome Instruments). The specific surface area was calculated by the modified Brunauer-Emmet-Teller (BET) method. The pore size distributions and the pore volume were analyzed from the adsorption branch isotherms by density functional theory (DFT) method. Moreover, the total pore volume (V_t) was estimated from the amount adsorbed at a relative pressure P/P_0 of 0.990. The micropore volume (V_{mic}) and micropore surface area (Smic) were determined by the t-plot theory. Raman spectra were acquired with a Jobin-Yvon HR 800 spectrometer. X-ray photoelectron spectroscopy (XPS) measurements were performed on a Thermo Fisher Scientific (Escalab 250xi, USA). Fourier transform infrared (FT-IR) spectra were recorded on a Thermo Scientific Nicolet iS 50 spectrometer.

Electrochemical measurements

Electrodes were fabricated by mixing electroactive material, carbon black and polyvinylidene fluoride in a mass ratio of 80: 10: 10 in N-methylpyrrolidone to obtain slurry. Then the slurry was pressed onto the nickel foam current collector (1 cm × 1 cm) and dried at 80 ℃ for 12 h. The mass loading of the electrode materials was ~3 mg cm^{-2}. Electrochemical characterization was carried out in a conventional three-electrode cell with 0.5 M Na_2SO_4 as the electrolyte. Platinum foil and Ag/AgCl were used as the counter and reference electrodes, respectively. All electrochemical measurements were conducted with a CHI 760E electrochemical workstation (Shanghai Chenhua Instrument Co. Ltd, China).

The symmetric supercapacitor was built with a glassy fibrous separator and performed in a two-electrode cell in 0.5 M Na_2SO_4 aqueous solution. The specific capacitance of electrodes were calculated from the charge/discharge curves by the following equation:

$$C_{sp} = I \times \triangle t/m \times \triangle V \qquad (1)$$

Where C_{sp} (F g^{-1}) is specific capacitance based on the mass of the active carbons, I is the current density and ΔV is the potential change within the discharge time Δt, Δt is discharge time measured in seconds, m (g) is the mass of electroactive materials and ΔV is potential window (V).

The key parameters of the supercapacitors, energy density (E) and power density (P) were calculated by equations:

$$E = 0.5C_{sp}V^2 \qquad (2)$$

$$P = E/t \qquad (3)$$

where t is the discharge time (s).

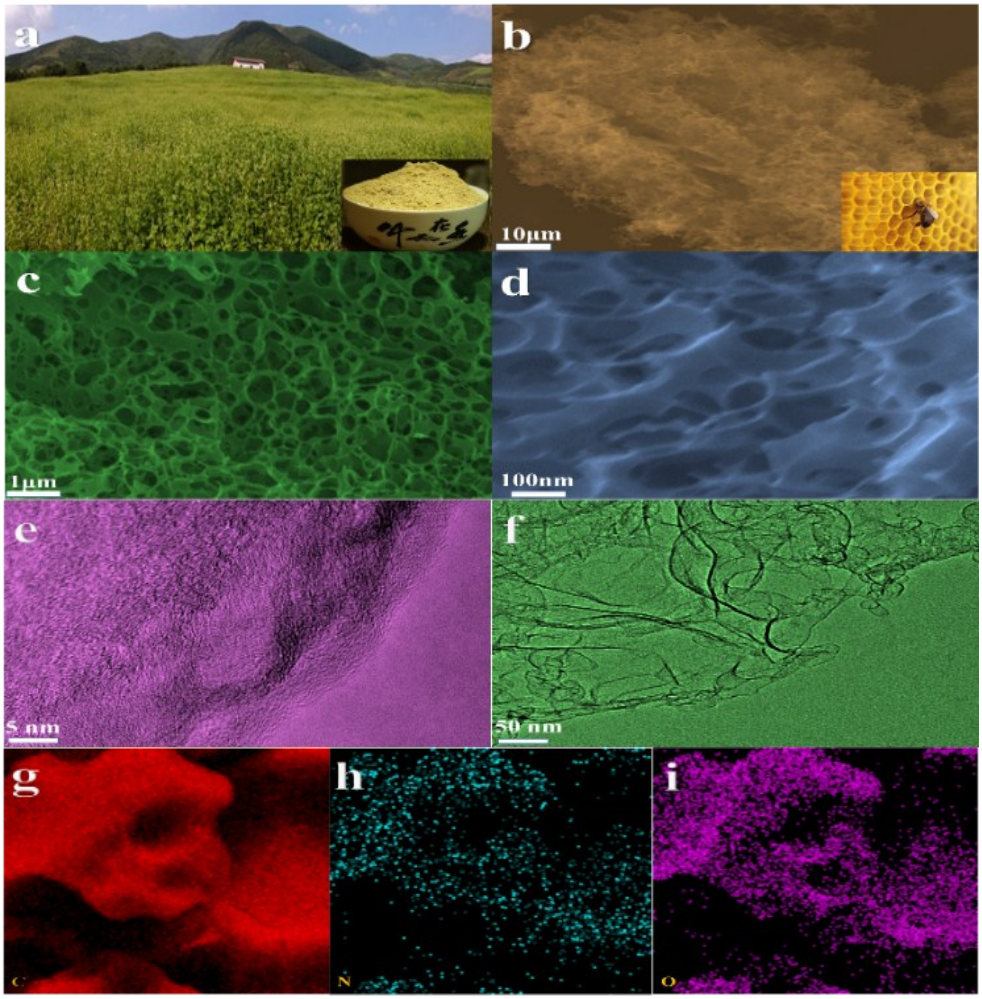

Figure S1 (a) Photograph of buckwheat field, the inset is buckwheat flour. (b) SEM image of HPC-2, the inset is the photograph of a honeycomb. (c, d) High resolution SEM images of HPC-2. (e, f) TEM image of HPC-2, and corresponding elemental mapping images of C (g), N (h) and O (i).

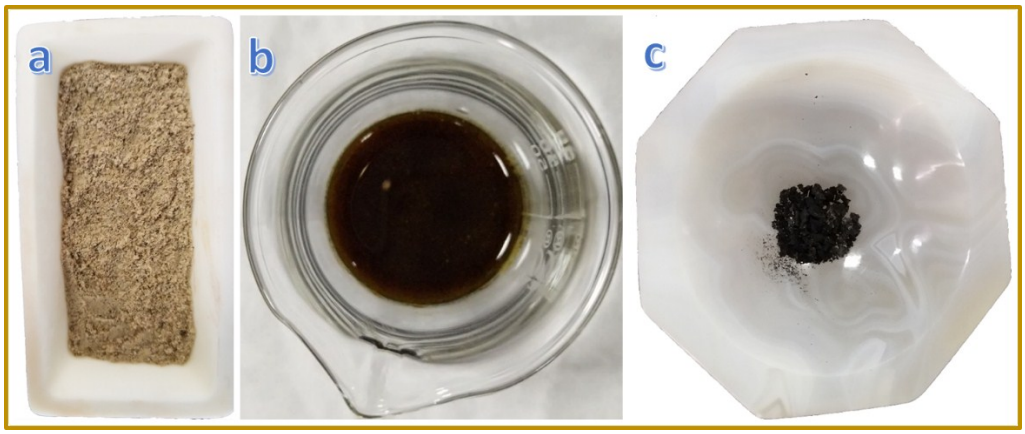

Figure S2 Digital photographs of (a) buckwheat flour, (b) sol-gel, (c) HPC.

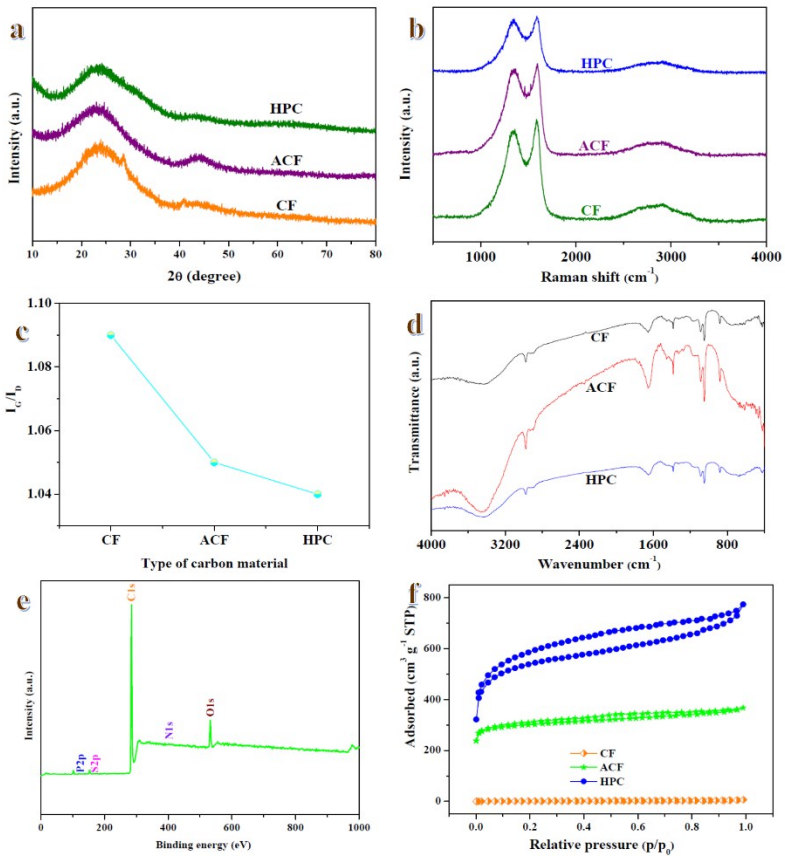

Figure S3 (a) XRD patterns of CF, ACF and HPC-2. (b) Raman spectrum of CF, ACF, HPC-2. (c) Ratio of integrated intensities of G- and D bands (I_D/I_G) of CF, ACF, HPC-2. (d) FT-IR spectra of CF, ACF, HPC-2. (e) XPS survey spectrum of HPC-2. (f) N_2 adsorption/ desorption isotherms of CF, ACF and HPC-2.

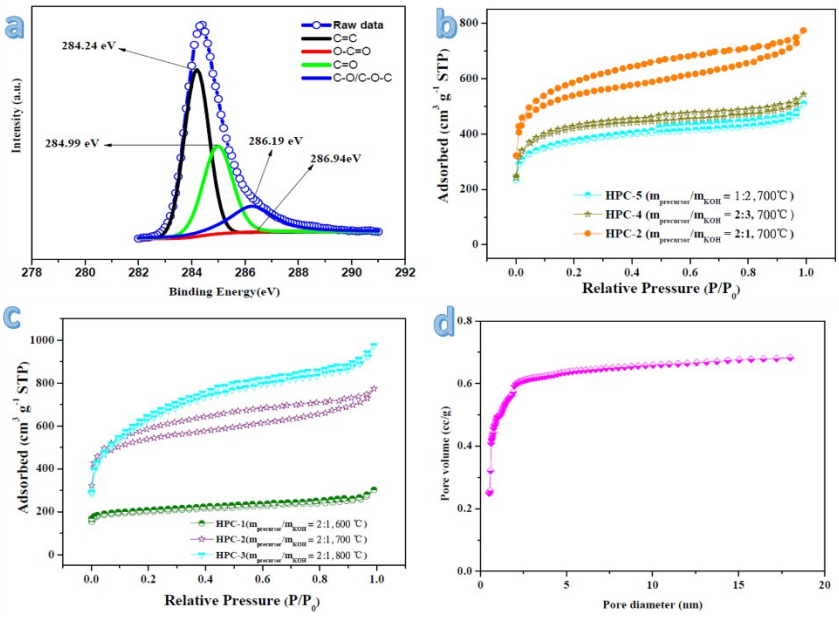

Figure S4 (a) High resolution C 1s of the HPC sample. (b) N_2 adsorption/desorption isotherms of the HPC samples prepared with different mass ratios of precursor/KOH at same temperature. (c) N_2 adsorption/ desorption isotherms of the HPC samples with same ratios of precursor/KOH (2:1) at

different temperature. (d) The pore size distribution of HPC-2.

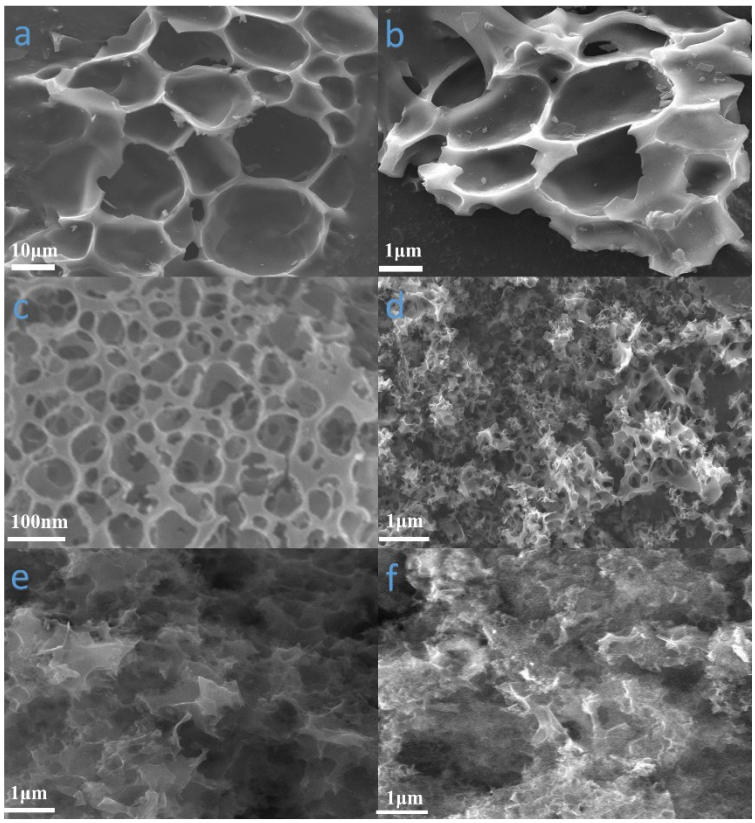

Figure S5 (a) SEM image of CF. (b) SEM image of ACF. (c) SEM images of HPC-2 ($m_{precursor}/m_{KOH}$ =2:1, 700 ℃) (d) SEM images of HPC-5 ($m_{precursor}/m_{KOH}$ =1:2, 700 ℃). (e) SEM images of HPC ($m_{precursor}/m_{KOH}$ =2:1, 600 ℃). (f) SEM images of HPC ($m_{precursor}/m_{KOH}$ =2:1, 800 ℃).

Table S1 Summary of BET characteristics of activated carbons.

Sample	S_{BET}[a] ($m^2\ g^{-1}$)	V_{tot}[b] ($cm^3 g^{-1}$)	S_{mi}[c] ($m^2 g^{-1}$)	S_{me}[d] ($m^2 g^{-1}$)	S_{ma}[e] ($m^2 g^{-1}$)	V_{mi}[f] ($cm^3\ g^{-1}$)	V_{me}[g] ($cm^3 g^{-1}$)	V_{ma}[h] ($cm^3 g^{-1}$)
CF	3.356	0.007	0.0535	3.243	0.0595	0.00005	0.0069	0.00005
ACF	1146	0.507	115.4	43.2	987.4	0.075	0.086	0.346
HPC-1	851	0.398	41.32	47.08	762.635	0.0295	0.1255	0.243
HPC-2	1541	1.052	700.11	149.8	691.09	0.459	0.299	0.294
HPC-3	1555	1.337	812.97	324.6	417.43	0.555	0.612	0.17
HPC-4	1137	0.731	482.77	68.1	586.13	0.319	0.157	0.255
HPC-5	1211	0.683	373	82.2	755.8	0.244	0.186	0.253

[a] S_{BET}: BET surface area; [b] V_{tot}: total volume; [c] S_{mi}: micropore surface area; [d] S_{me}: mesopore surface area; [e] S_{ma}: macropore surface area; [f] V_{mi}: micropore volume; [g] V_{me}: mesopore volume; [h] V_{ma}: macropore volume.

In this work, the Brunauer–Emmett–Teller (BET) method is used to determine surface area, which is fundamentally based on gas adsorption theory and has been presented in detail in literatures[1-2], while the BET equations stored in the instrument can be conveniently used to analyze the pore structure and calculated the surface area. The DFT (differential functional theory) method is applied to the N_2 adsorption isotherms to determine the pore size distribution and the pore volume[2-5]. The micropore (V_{micro}) and mesopore (V_{meso}) volumes were calculated using the Dubinin−Radushkevich analysis.

References

1. Kenneth Sing: Colloids and Surfaces A: Physicochemical and Engineering Aspects. 187-188 (2001) 3-9.
2. Shi-Yu Lu, Meng Jin, Yan Zhang, Yu-Bing Niu, Jie-Chang Gao, and Chang Ming Li: Chemically Exfoliating Biomass into a Graphene-like Porous Active Carbon with Rational Pore Structure, Good Conductivity, and Large Surface Area for High-Performance Supercapacitors. Adv. Energy Mater. (2017) 1702545.
3. Encarnación Raymundo-Piñero, Martin Cadek, and François Béguin: Tuning Carbon Materials for Supercapacitors by Direct Pyrolysis of Seaweeds. Adv. Funct. Mater. 19 (2009) 1032-1039.
4. Xian-jun Wei, Yong-bin Li, Shu-yan Gao: Biomass-derived interconnected carbon nanoring electrochemical capacitors with high performance in both strongly acidic and alkaline electrolytes. J. Mater. Chem. A, 5 (2017) 181-188.
5. Lu Wei, Marta Sevilla, Antonio B. Fuertes, Robert Mokaya, and Gleb Yushin: Hydrothermal Carbonization of Abundant Renewable Natural Organic Chemicals for High-Performance Supercapacitor Electrodes. Adv. Energy Mater. 1(2011)356-361.